

Electronic Supplementary Material (ESI) for Journal of Materials Chemistry A

Long-range Exciton Diffusion in Non-Fullerene Acceptors and Coarse Bulk Heterojunctions Enable Highly Efficient Organic Photovoltaics

Muhammad T. Sajjad,^{*a,b} Arvydas Ruseckas,^a Lethy Krishnan Jagadamma,^a Yiwei Zhang^a and Ifor D. W. Samuel^{*a}

^aOrganic Semiconductor Centre, SUPA, School of Physics and Astronomy, University of St Andrews, St. Andrews, KY16 9SS, United Kingdom.

* Prof. Ifor Samuel: idws@st-andrews.ac.uk

^bLondon Centre for Energy Engineering, School of Engineering, London South Bank University, 103 Borough Rd, London, SE1 0AA, United Kingdom

* Dr Muhammad Tariq Sajjad: sajjad@lsbu.ac.uk

Measurements of exciton diffusion in NFAs using volume quenching and analysis

Small concentrations of DR3TBDDT molecules were dispersed in the volume of electron acceptor films and PL decays were measured. Decays get faster with increasing the concentration of a quencher.

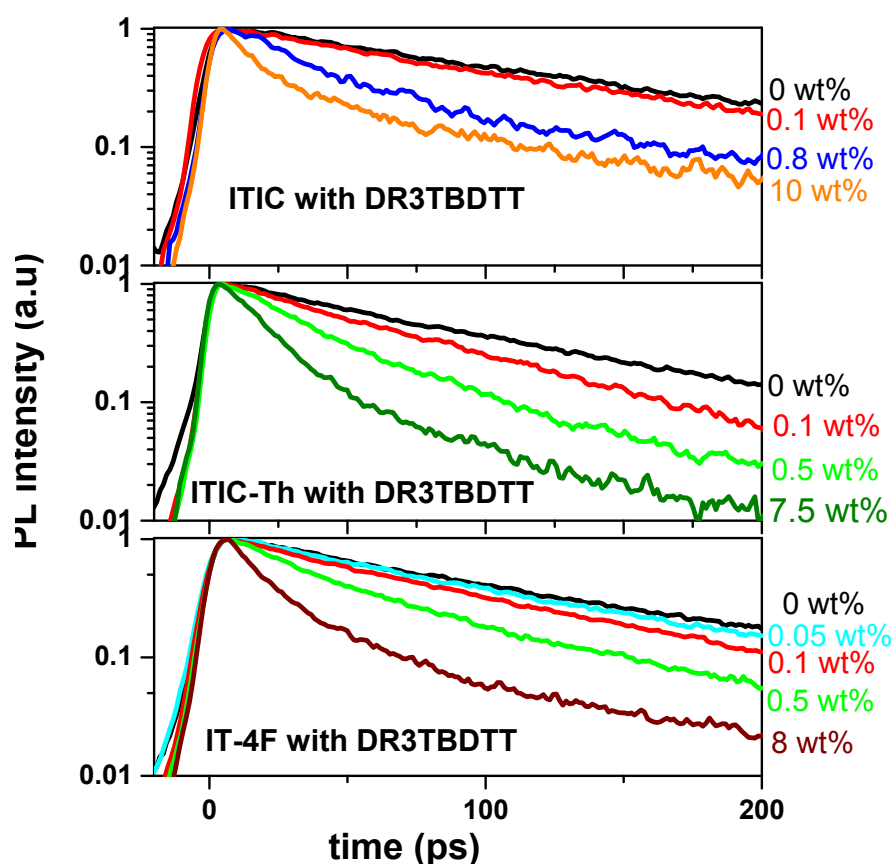


Figure S1: Photoluminescence decays in films of ITIC derivatives doped with small known concentrations of DR3TBDDT molecules dispersed in the films.

In order to check the homogenous dispersion of the quencher i.e. to establish a cluster-free regime, we investigated a range of quencher concentrations and measured the rate of quenching for each concentration (Figure S2). The rate of quenching obtained from the slope of $\ln(\text{PL ratio})$ is plotted in Figure S2b. There is a clear change of regime at higher concentration. For exciton diffusion measurements, we only use the linear regime (i.e. low concentration as shown in the inset of Figure S2b).

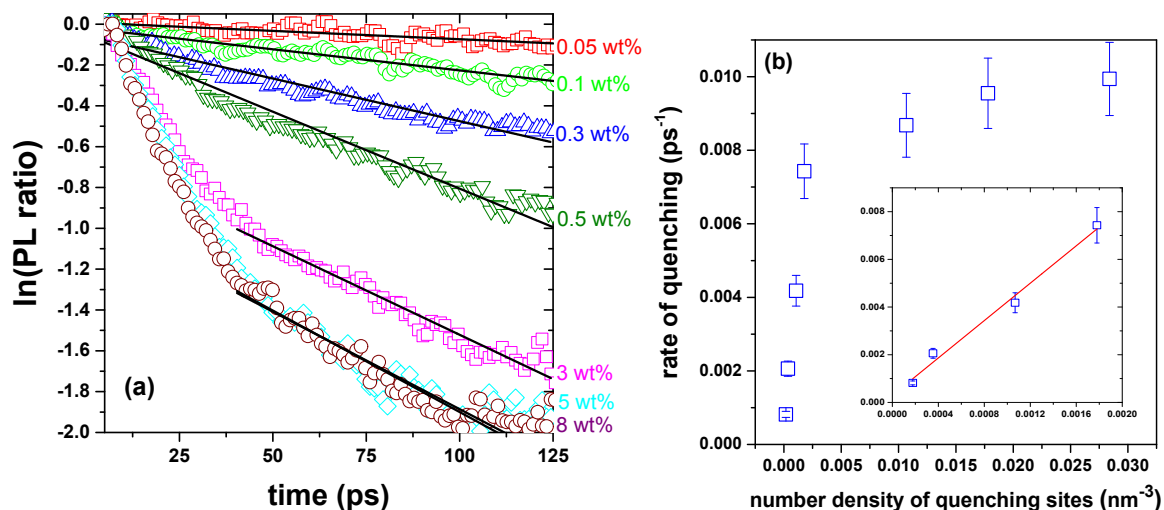


Figure S2: (a) The natural logarithm of the ratio of the PL decays in films of IT-4F doped with different concentrations of the quencher to the PL of the neat films without a quencher plotted on a linear time axis. The rate of quenching was obtained from the slope (black lines) of $\ln(\text{PL ratio})$. (b) rate of PL quenching vs concentration of quenching sites, showing linear dependence at low concentration of the quencher (see inset) and a clear deviation from the linear regime at high concentration.

The time-resolved PL intensity is proportional to the density of singlet excitons which in a neat film N_{neat} can be described by the rate equation

$$\frac{dN_{neat}}{dt} = -k N_{neat} \quad (S1)$$

In films doped with a dispersed quencher the density of singlet excitons N_{doped} has an additional decay path with a rate constant k_q

$$\frac{dN_{doped}}{dt} = -k N_{doped} - k_q N_{doped} \quad (S2).$$

Introducing a new variable $g(t) = N_{doped}/N_{neat}$ which in this case is the same as the ratio of time-resolved PL intensities $g(t) = PL_{doped}/PL_{neat}$ and substituting into Equations S1 and S2 we get^{1,2}

$$k_q = -\frac{d}{dt} \ln [g(t)] \quad (S3).$$

We analyzed these PL decays using the formula developed by Gösele et al for the case of diffusion-mediated Förster resonance energy transfer (FRET) to dispersed quenchers^{3,4}

$$\ln [g(t)] = -4\pi D r_F Q t - \frac{4}{3} \pi Q \left[\frac{\pi R_0^6 t}{\tau} \right]^{1/2} \quad (S4)$$

where D is the diffusion coefficient, Q is the density of quenchers, τ is the exciton lifetime in the host material, R_0 is the Förster radius for FRET to the quencher and

$$r_F = 0.676 \left[\frac{R_0^6}{D\tau} \right]^{1/4} \quad (S5).$$

At high concentrations of dispersed quenchers all excitons are close enough to the quencher, so that direct FRET to the quencher dominates the decays and the natural logarithm of the PL ratio is proportional to the square root of time

$$\ln [g(t)] \approx -\frac{4}{3}\pi Q \left[\frac{\pi R_0^6 t}{\tau} \right]^{1/2} \quad (S6)$$

We use the decays of PL ratio $g(t)$ at high quencher concentrations and Equation S6 to determine R_0 and then we use Equations S4 and S5 to fit the $\ln[g(t)]$ decays at low quencher concentrations with D as a fitting parameter.

Measurement of annihilation-free decay

In order to measure the PL under annihilation-free conditions, we measure PL at an excitation density intensity two orders of magnitude lower than for the annihilation experiments shown in **Figure 3** and **S3**. We also study the intensity dependence of the response and make sure that different intensities give the same shape of PL decay, as shown below.

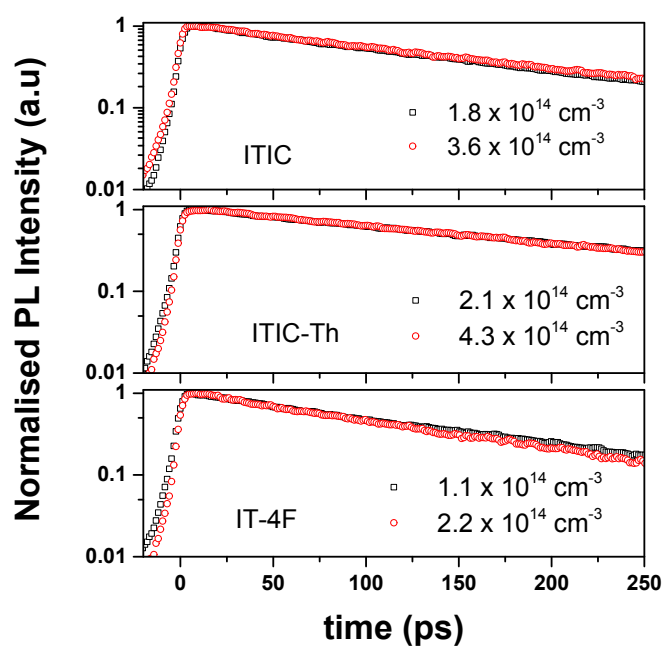


Figure S3: Time-resolved PL decays of neat films of NFAs measured at very low excitation densities

Fitting exciton decay at low excitation density

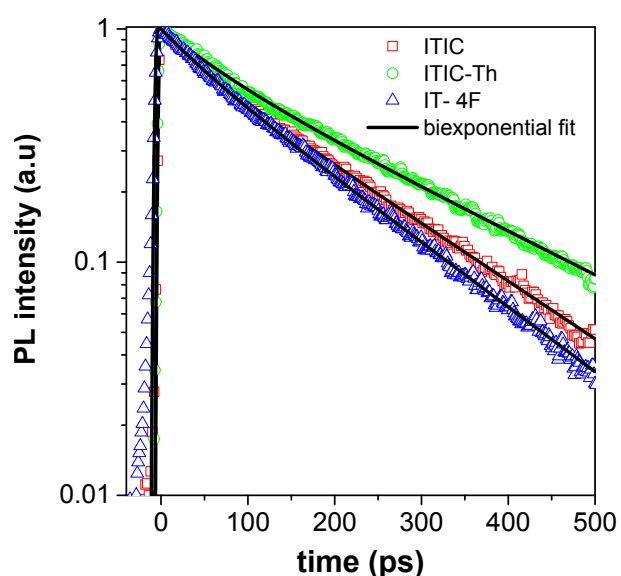


Figure S4: Time-resolved PL decays of neat films of NFAs measured at low excitation density. The PL decays were fitted with two exponential functions. Solid black lines are fits to experimental data.

The PL decay at very low excitation density ($<10^{15} \text{ cm}^{-3}$) was normalised by dividing by its maximum value and then fitted with a sum of two exponential functions i.e. $a_1 e^{-\frac{t}{\tau_1}} + a_2 e^{-\frac{t}{\tau_2}}$. The fitted results are shown in **Figure S4** and fitted parameters are given in Table S1.

Table S1: Parameters obtained by fitting PL decays of NFAs shown in figure S4 with two exponential functions.

Sample	a_1	τ_1 (ps)	a_2	τ_2 (ps)
ITIC	0.22	45	0.78	175
ITIC-Th	0.26	69	0.74	233
IT-4F	0.19	49	0.81	157

Determination of annihilation rate constant using linear fits

Here we show a simple alternative analysis of our annihilation data.

The annihilation equation with instantaneous generation rate

$$\frac{dN}{dt} = -kN(t) - \gamma N^2 \quad (S7)$$

can be solved for time-independent γ to obtain

$$N(t) = \frac{N(0)\exp(-kt)}{1 + \frac{\gamma}{k}[1 - \exp(-kt)]} \quad (S8)$$

where $N(0)$ is the initial exciton density.

Equation S8 can then be rearranged into the linear form

$$\frac{1}{N(t)} = \left(\frac{1}{N(0)} + \frac{\gamma}{k} \right) \exp(kt) - \frac{\gamma}{k} \quad (S9)$$

We obtained $N(t)$ from the PL decays and $N(0)$ from the excitation energy density. Then we plotted $\frac{1}{N(t)}$ against $\exp(kt)$ as shown in **Figure S5**. The time-independent annihilation rate γ was determined from the slope of the linear fit. We obtained values for γ of $(1.0 \pm 0.2) \times 10^{-8} \text{ cm}^3/\text{s}$ for ITIC, $(1.4 \pm 0.1) \times 10^{-8} \text{ cm}^3/\text{s}$ for ITIC-Th and $(1.2 \pm 0.1) \times 10^{-8} \text{ cm}^3/\text{s}$ for IT-4F. These values are consistent with the values deduced in the main paper.

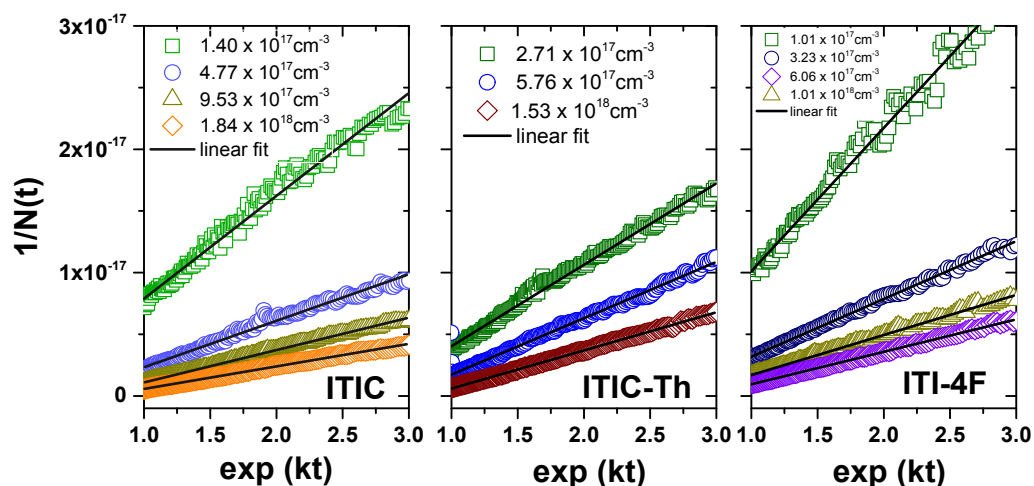


Figure S5: Inverse exciton density vs $\exp(kt)$ of NFA films with their associated linear fits.

Measurement of exciton diffusion in PTB7-Th using volume quenching

Small concentrations of ITIC or IT-4F were dispersed in the volume of PTB7-Th films and PL decays were measured. The fluorescence decay in a neat PTB7-Th film shows $1/e$ decay time of $\tau=240$ ps. Decays get faster with increasing the concentration of the quencher.

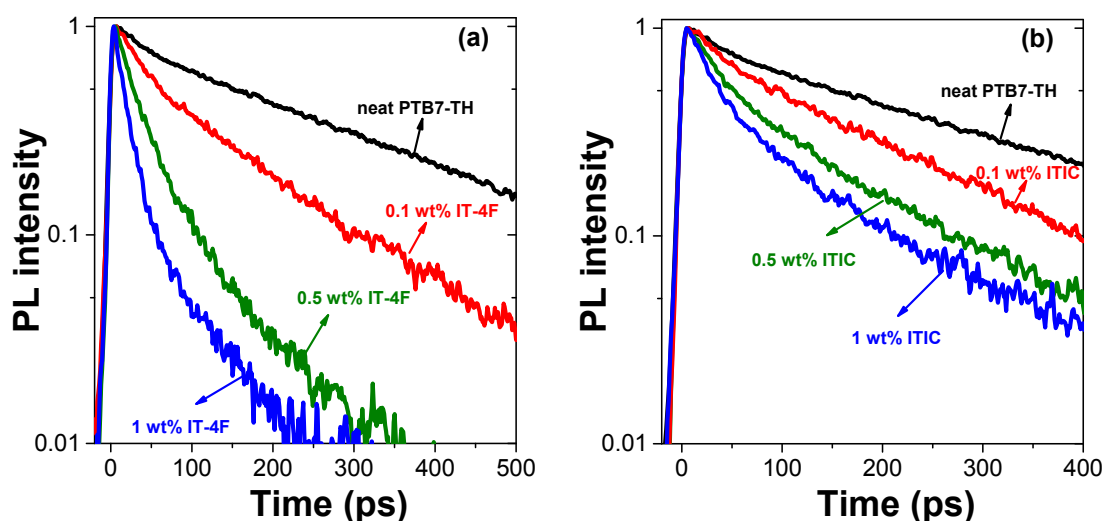


Figure S6: Normalised PL decays of PTB7-Th films doped with low concentrations (0.1wt%, 0.5wt% and 1wt%) of IT-4F (a) and ITIC (b). Laser wavelength of 515nm was used to excite the films.

There is a strong overlap between the fluorescence spectrum of PTB7-Th and absorption spectra of the ITIC and IT-4F quenchers and (Shown in Figure S7), so there is a chance of significant direct quenching due to FRET, especially at high quencher concentration. The PL quenching of PTB7-Th is a combined effect of direct quenching due to Förster process (FRET) and diffusion-mediated quenching.

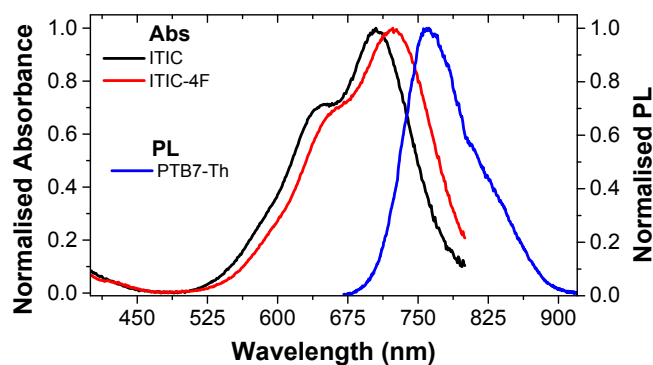


Figure S7: Normalised absorption spectra of NFAs and PL emission of PTB7-Th.

By fitting the decays with 1 wt% of quencher we get $R_o = 5.4 \text{ nm}$ for FRET from PTB7-Th to IT-4F and $R_o = 3.8 \text{ nm}$ to ITIC (**Figure S8a**). Then the PL decays at low quencher concentrations were fitted using Equation S4 with the diffusion coefficient D as a fitting parameter (**Figure S8b**). This gives a diffusion coefficient of $(1.0 \pm 0.1) \times 10^{-3} \text{ cm}^2/\text{s}$ in PTB7-Th films and a 3D diffusion length of 12 nm using $L_{3D} = \sqrt{6D\tau}$.

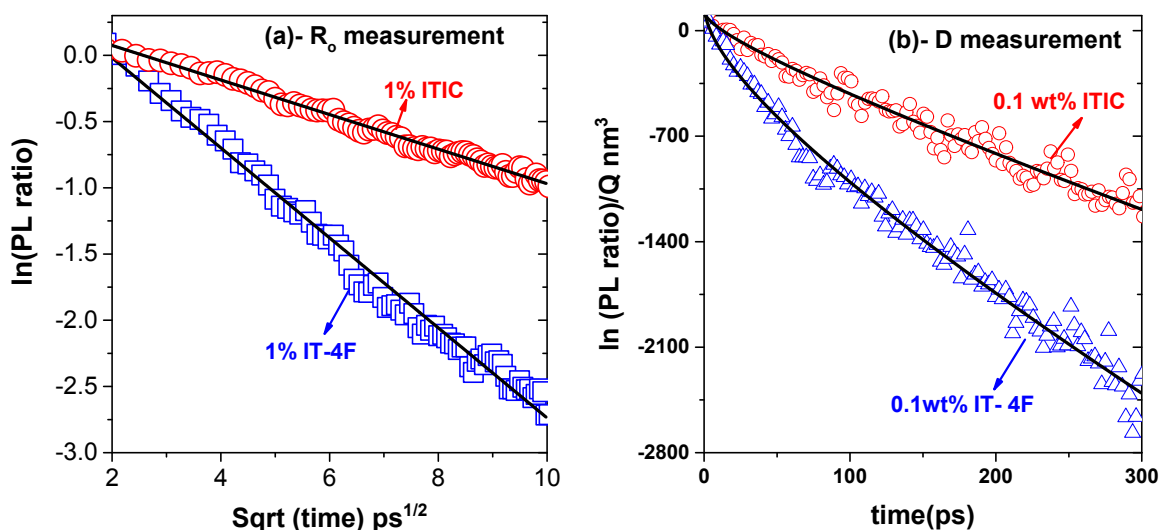


Figure S8: (a) The natural logarithm of the ratio of the PL with a higher concentration of quencher (1 wt%) to the PL without a quencher. The black lines are fits to the experimental data using equation S6, with the Förster radius, R_o , as the fitting parameter. (b) The natural logarithms of the ratio of the PL with a lower concentration of quencher (0.1wt%) to the PL without a quencher. The black lines are fits to the experimental data using equation S4, with D as the fitting parameter.

Ionisation potentials and electron affinities

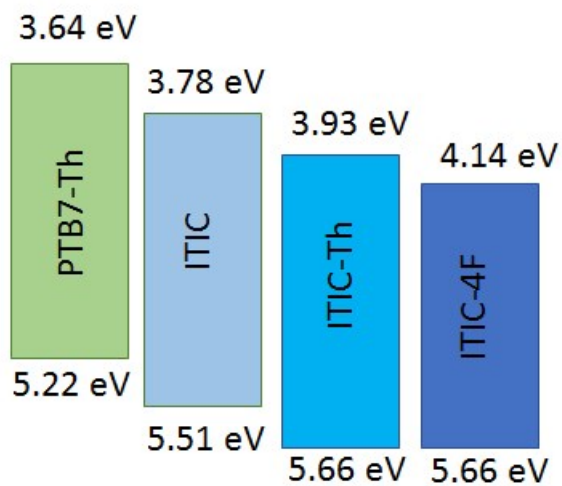


Figure S9: Ionisation potentials and electron affinities of electron donor and acceptor materials which we used to make solar cells. The values are taken from Reference 5 for ITIC derivatives and from Reference 6 for PTB7-Th.

Determination of ideality factor (n)

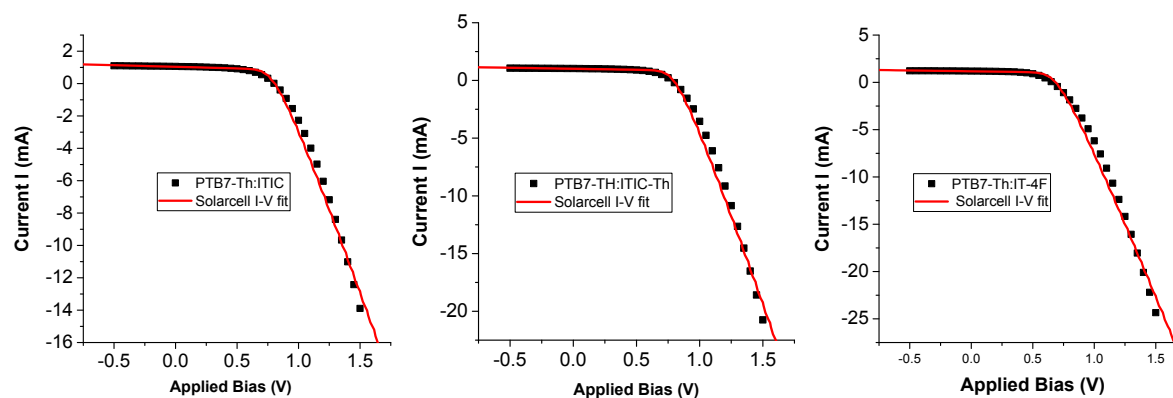


Figure S10: *I-V* curves of solar cell blends fitted with equation 3 to obtain the ideality factor n . The values of n obtained are 1.53 ± 0.41 for PTB7-Th:ITIC, 1.43 ± 0.34 for PTB7-Th:ITIC-Th and 1.55 ± 0.39 for PTB7-Th:IT-4F

PL spectra of neat films and Blends

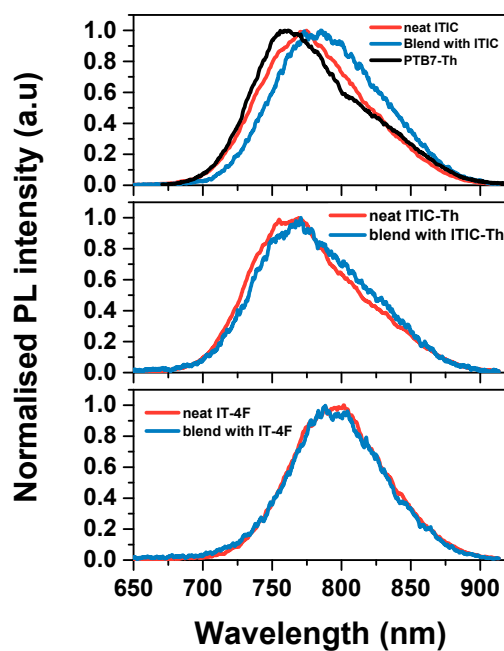


Figure S11: Time-integrated PL spectra of neat films of PTB7-Th and acceptors, and of photovoltaic blends used to make devices.

Time-resolved PL spectra of Blends

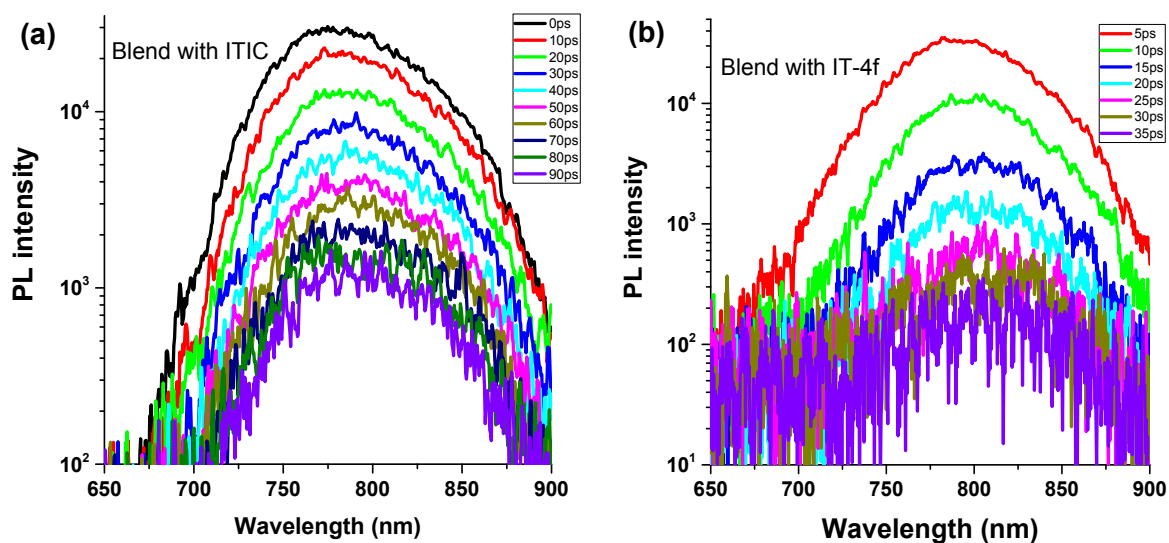


Figure S12: Time-resolved PL spectra of photovoltaic blends of PTB7-Th with ITIC (a) and PTB7-Th with IT-4f (b).

AFM image of PTB7-Th:ITIC blend

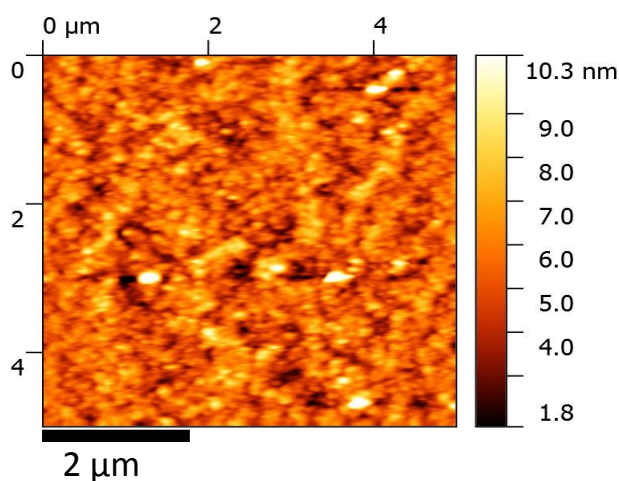


Figure S13: AFM image of PTB7-Th : ITIC blend indicating that domains are approximately spherical

References

1. M. Yokota and O. Tanimoto, *Journal of the Physical Society of Japan*, 1967, **22**, 779-784.
2. A. Ruseckas, P. E. Shaw and I. D. W. Samuel, *Dalton Transactions*, 2009, DOI: 10.1039/B912198F, 10040-10043.
3. U. Klein, R. Frey, M. Hauser and U. Gösele, *Chem. Phys. Lett.*, 1976, **41**, 139-142.
4. U. Gösele, M. Hauser, U. Klein and R. Frey, *Chem. Phys. Lett.*, 1975, **34**, 519-522.
5. A. Wadsworth, M. Moser, A. Marks, M. S. Little, N. Gasparini, C. J. Brabec, D. Baran and I. McCulloch, *Chemical Society Reviews*, 2019, **48**, 1596-1625.
6. S. H. Liao, H. J. Jhuo, Y. S. Cheng and S. A. Chen, *Advanced Materials*, 2013, **25**, 4766-4771.